Journal of Hazardous Materials 394 (2020) 122573

Contents lists available at ScienceDirect

Journal of Hazardous Materials

journal homepage: www.elsevier.com/locate/jhazmat

The pollution profiles and human exposure risks of chlorinated and brominated PAHs in indoor dusts from e-waste dismantling workshops: Comparison of GC–MS, GC–MS/MS and GC × GC–MS/MS determination methods

Jian Tang[a], Shengtao Ma[a,b], Ranran Liu[a], Congcong Yue[a], Guiying Li[a,b], Yingxin Yu[a], Yan Yang[a,b], Taicheng An[a,*]

[a] Guangdong Key Laboratory of Environmental Catalysis and Health Risk Control, Guangzhou Key Laboratory of Environmental Catalysis and Pollution Control, School of Environmental Science and Engineering, Institute of Environmental Health and Pollution Control, Guangdong University of Technology, Guangzhou, 510006, China
[b] Synergy Innovation Institute of GDUT, Shantou, 515100, China

GRAPHICAL ABSTRACT

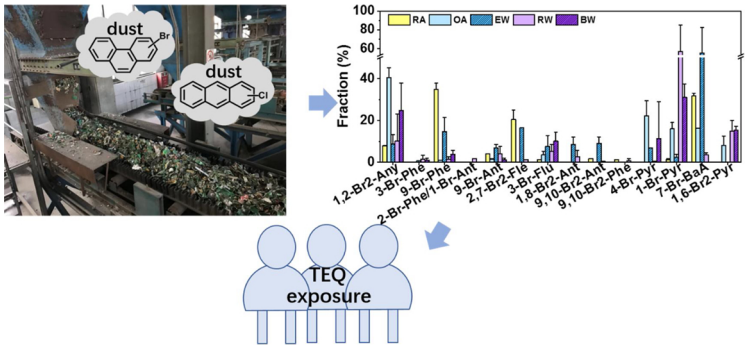

ARTICLE INFO

Editor: R Teresa

Keywords:
Chlorinated PAHs
Brominated PAHs
Indoor dust
E-waste
Health risk

ABSTRACT

The toxicities of some chlorinated and brominated polycyclic aromatic hydrocarbons (X-PAHs) are higher than their corresponding parent PAHs. However, the identification and quantitation of X-PAHs in environment are still changeable and limitedly reported. To develop a robust method for routine analysis of X-PAHs in environmental samples, the determination of 34 X-PAHs was performed and compared using different instruments, including gas chromatography-mass spectrometry (GC–MS), gas chromatography-tandem mass spectrometry (GC–MS/MS) in both electron ionization (EI) and negative chemical ionization (NCI) modes, and comprehensive two-dimensional gas chromatograph-tandem mass spectrometer (GC × GC–MS/MS). GC-EI-MS/MS possessed the highest sensitivity with method detection limits of 2.00–40.0 and 2.00–20.0 pg/g dry weight (dw) for Cl-PAHs and Br-PAHs, respectively. This validated method was then applied to analyze X-PAHs in indoor dusts from a typical e-waste dismantling workshop, and the concentrations of Σ_{18}Br-PAHs (8.80–399 ng/g dw) were higher than Σ_{16}Cl-PAHs (7.91–137 ng/g dw). The toxicity equivalency quantities (TEQs) of Cl-PAHs at e-waste dismantling workshop and Br-PAHs at raw materials crushing workshop showed

* Corresponding author.
E-mail address: antc99@gdut.edu.cn (T. An).

https://doi.org/10.1016/j.jhazmat.2020.122573
Received 24 January 2020; Received in revised form 5 March 2020; Accepted 19 March 2020
Available online 20 March 2020

the highest values of 176 and 453 pg·TEQ/g, respectively. Cl-PAHs and Br-PAHs posed a potential health risk to workers through dust ingestion in workshops. Further attention should be payed to the formation mechanism of X-PAHs and the health risk.

1. Introduction

Chlorinated and brominated polycyclic aromatic hydrocarbons (X-PAHs) are a group of organics with one or more halogen substituents on the aromatic rings of corresponding parent polycyclic aromatic hydrocarbons (PAHs). They can be released into the environment during automobile emission, waste incineration, as well as electronic waste (e-waste) dismantling process (Ohura et al., 2016; Sun et al., 2013). Due to the ubiquity of X-PAHs in various environmental matrices such as sediments, dusts, solids, air particles, fly ashes, and snows (Fan et al., 2017; Haglund et al., 1987; Horii et al., 2009; Jin et al., 2020; Ma et al., 2013; Sankoda et al., 2013), people can be exposed to X-PAHs through various exposure pathways. Currently available studies indicated that X-PAH isomers could exhibit toxicity by combining with aryl hydrocarbon receptor (AhR) in rat hepatoma cells and breast cancer cells (Horii et al., 2013; Jin et al., 2017a; Ohura et al., 2010; Takeshi et al., 2007). As reported, the toxicities of some X-PAHs are even higher than the corresponding parent PAHs and would induce adverse estrogen-related actions (Horii et al., 2013; Ohura et al., 2007). However, researches on the occurrences of X-PAHs in the living environment are still insufficient and have caused limited attention only in recent years, owing to their large number of isomers and difficulty in accurate quantification, as well as complex environmental matrices (Jin et al., 2017a; Nishimura et al., 2017).

Currently, the determination of X-PAHs in the environment present several analytical challenges such as the absence of high-resolution mass spectrometry in many laboratories and the absence of commercially available authentic standards of X-PAHs for the identification and quantification (Horii et al., 2008; Ohura, 2007; Ohura et al., 2009). To date, a number of methods were developed and applied to analyze X-PAHs. Among these methods, gas chromatography-mass spectrometry operated in electron capture negative ionization (GC-ECNI-MS) (Gonzales, 2011; Haglund et al., 1987; Nilsson and Oestman, 1993) and electron ionization (GC-EI-MS) (Horii et al., 2008; Ma et al., 2009) were the mostly frequently used methods (Sun et al., 2013). Gas chromatography combined with low resolution mass spectrometry (GC-LRMS) technique is usually employed the preferred instrumental analysis method to determine X-PAHs for many laboratories (Gonzales, 2011; Haglund et al., 1987; Horii et al., 2008; Ma et al., 2009; Nilsson and Oestman, 1993) as compared with gas chromatography-high resolution mass spectrometry (GC-HRMS) technique. Recently, methods based on high resolution mass spectrometry have been developed and applied (Nishimura et al., 2017; Ohura et al., 2008, 2009). Using HRMS would obviously give more confidence to the qualification and quantification of X-PAHs (Jin et al., 2017a). However, the complex in operation and maintenance makes the HRMS not suitable for routine analysis. Furthermore, although GC-HRMS can significantly increase the selectivity for specific congener determination as compared with LRMS with limited resolution, GC-LRMS was routinely and frequently applied to analyze X-PAHs (Mo et al., 2013). Recently, although only limited data have been reported, 20 Cl-PAHs and 11 Br-PAHs have been successfully detected with higher sensitivity and selectivity using gas chromatography-tandem mass spectrometry (GC–MS/MS) than gas chromatography-mass spectrometry (GC–MS) (Ohura et al., 2015, 2013). To date, some researchers also found higher peak capacity with two-dimensional chromatography (GC × GC) than GC for analyzing X-PAHs, therefore, GC × GC could be applied to separate analytes and complex organic mixtures from unresolved complex matrices (Miren et al., 2014; Petros et al., 2015). Overall, due to high cost of HRMS, which cannot be universally applied to routine analysis, and the low resolution and sensitivity of LRMS, current analytical methods have limitations for the separation and determination of X-PAHs isomers. Thus, there is a great challenge for analysis and quantify X-PAHs, making it difficult to study the pollution profiles and toxic effects of X-PAHs in the environment from different sources.

There are many possible sources of X-PAHs released into the environment. Vehicle emissions (Haglund et al., 1987; Ohura, 2007), waste incineration (Horii et al., 2008), and e-waste recycling (Gonzales, 2011; Ma et al., 2009; Nishimura et al., 2017) might be considered as primary emission sources for X-PAHs. In addition, the use of scrap copper as raw material or the addition of coal or heavy oil as reductant in secondary copper smelters was found to contribute to the elevated formation and emission of X-PAHs (Jin et al., 2017b). Metallurgical industries were also found to be important sources of atmospheric emissions of the emerging organic contaminants X-PAHs (Xu et al., 2018). In dusts from e-waste recycling facility, high levels of Cl-PAHs were determined, which have higher toxic equivalency quotients (TEQs) than their parent PAHs (Ma et al., 2009). In addition, high concentrations of total Cl-PAHs and Br-PAHs were also determined in e-waste opening burning soils (Nishimura et al., 2017), which were higher than those in soils from an urbanized region of Shenzhen, China (Ni and Zeng, 2012). Due to high exposure potential to X-PAHs, the pollution profiles of X-PAHs in the e-waste recycling areas need to be investigated to facilitate the human exposure risk assessment.

Therefore, to develop a method suitable for routine analysis of X-PAHs with relative easier in operation and maintenance as well as cheaper in cost, GC–MS, GC–MS/MS and GC × GC–MS/MS with different ion sources were compared. The main objectives of this study were to apply the accurate analytical method for separation and quantification of X-PAHs, to determine the pollution profiles of X-PAHs in indoor dusts from e-waste dismantling workshops, and to estimate the human exposure risk of X-PAHs via dust ingestion. The present developed analysis method would provide a reference for the accurately qualitative and quantitative analysis of X-PAHs.

2. Materials and methods

2.1. Chemicals

Deuterated PAH standard mixtures, including naphtalene-d_8, acenaphtene-d_{10}, chrysene-d_{12}, phenanthrene-d_{10}, and perylene-d_{12}, were served as recovery surrogate standards, which were obtained from AccuStandard (New Haven, CT, USA). Standard Reference Material 2585 Organic Contaminants in House Dust were purchased from NIST (Gaithersburg, MD, USA). SRM 2585 was prepared from house dusts collected from homes, cleaning services, and hotels in several states in the USA during 1993 and 1994, and was widely used for the method development and validation for several classes of organic contaminants including PBDEs, PAHs and PCBs in house dust or similar sample matrixes (NIST, 2010; Stapleton et al., 2006). Although the certified values of X-PAHs were unknown, the method performance for the analysis of PAHs can provide a valuable reference based on their similarity of chemical properties. In addition, the characterization of X-PAHs in SRM 2585 in the present study may be useful for future comparisons of methods developed by other studies. Other chemicals as well as materials were described in Supporting Information (SI) and the detailed information of the 34 X-PAHs is listed in Table S1.

2.2. Sample collection and pretreatment

Fifteen indoor dust were sampled from a typical e-waste dismantling industrial park (including an office building area (OA, n = 2), e-waste dismantling workshop (EW, n = 5), raw materials crushing workshop (RW, n = 3), secondary copper blast furnace workshop (BW, n = 3)) and its surrounding area (a residential area (RA, n = 2)) in southern China (Fig. S1). The indoor dust samples were collected using a preclean soft-bristled brush from the surface of tables, furniture, windowsills (over 50 cm above the floor). To ensure a better sample homogeneity before analysis, the samples were sifted through a stainless-steel 100–200 mesh to get rid of large debris and particles. All samples collected were firstly aluminum foil-wrapped, put in a plastic bag and stored in freezer (−20 °C) until use. The sample pretreatment and analytical methods were based on our previous study (Chen et al., 2019). Details on the extraction and cleanup procedure of X-PAHs from the dust samples can be found in SI.

2.3. Instrumental analysis

Measurements of X-PAHs were performed on GC–MS and GC–MS/MS using a 7890B Series GC coupled with a 5977B Series MS (Agilent Technologies, USA) and a GC-2010 Plus coupled with 8040 triple quadrupole MS (Shimadzu, Japan), respectively. Three capillary columns (60 m length, 0.25 mm i.d. and 0.25 μm film thickness, Agilent Technologies, USA) with different polarity, including non-polar DB-5MS (5% Silphenylene Silicone co-polymer or Si-Arylene) column, medium polar DB-35MS (35 % Silphenylene Silicone co-polymer or Si-Arylene) column, and medium polar DB-17MS (50 % Silphenylene Silicone co-polymer or Si-Arylene) column, were tested to achieve the best separation on GC. Then the column presented the best separation performance was selected for further analysis with different mass spectrometers. The GC operating conditions were set as below.

High purity helium (> 99.999 %) was used as the carrier gas at a constant flow rate of 1 mL/min. Injection volume was 1 μL with a pulse splitless injection mode. The injector temperature was set at 280 °C. The oven temperature was programed as follows: initial 60 °C hold for 0.5 min; 10 °C/min to 200 °C (hold for 1 min); 3 °C/min to 250 °C (hold for 1 min); 5 °C/min to 280 °C (hold for 5 min); 10 °C/min to 300 °C, and finally hold for 20 min.

For the operating conditions of the MS and MS/MS, the quadrupole mass spectrometer was operated in electron ionization (EI) and negative chemical ionization (NCI) modes for both MS and MS/MS detection, although the same GC conditions were used. The transfer line, ion source, and MS quadrupole temperatures for EI mode were set at 300 °C, 230 °C and 150 °C, while they were 300 °C, 200 °C and 150 °C for NCI mode, respectively. EI electron energy was set at 70 eV. Argon (purity > 99.999 %) was used as MS/MS collision gas with a constant flow rate of 1.5 mL/min. NCI reagent gas was methane (purity > 99.999 %) at a constant flow rate of 2.0 mL/min.

The selected ion monitoring (SIM) mode on GC–MS with the two most abundant isotope clusters of each X-PAH isomer was used for the target determination. The determination of 34 target X-PAH isomers was conducted on GC–MS/MS in a multiple reaction monitoring (MRM) mode. The optimal precursor ions, productor ions, and collision energies for each X-PAH isomer in EI mode are listed in Table S2. The mass resolution was set at unit mass when work in MS mode; whereas the mass resolution of the precursor and the product ions were set in a wide mode to improve the sensitivity for MS/MS analysis.

To further verify and test the efficiency of separation with matrix interferences, a GC × GC approach was conducted using a Shimadzu GC-2010 Plus fitted with a SSM1810 modulator (J&X Technologies, China) and connected to an 8040 triple quadrupole MS (Shimadzu, Japan) in EI mode. The first-dimension column was a DB-35MS column (60 m × 0.25 mm × 0.25 μm, Agilent Technologies, USA), and the second-dimension column was a DB-17MS column (1.2 m length, 0.18 mm i.d. and 0.18 μm film thickness, Agilent Technologies, USA). Helium was used as carrier gas with a constant flow rate of 1.2 mL/min. The injection volume was 1 μL in splitless mode, and the temperature of injection port was set at 280 °C. The oven temperature was programed as follows: initial 60 °C hold for 0.5 min; 10 °C/min to 200 °C (hold for 1 min); 3 °C/min to 250 °C (hold for 1 min); 5 °C/min to 280 °C (hold for 5 min); 10 °C/min to 310 °C, and finally hold for 20 min. The modulation period was 4 s. The temperature of MS instrument transfer line was 300 °C, and the temperature of ion source was 230 °C. GC × GC data processing were performed with Canvas-2DGC® software (J&X Technologies, China).

Table 1
Retention times of individual standards of X-PAHs in different columns (60 m length, 0.25 mm i.d. and 0.25 μm film thickness) by GC-EI-MS.

Compounds	Retention time (min)		
	DB-5MS	DB-35MS	DB-17MS
9-Cl-Fle	21.759	25.289	24.268
2-F-Phe	22.417	25.903	24.776
5-Br-Ana	23.453	27.541	26.448
2-Br-Fle	25.565	30.217	28.830
9-Cl-Phe	27.540	32.685	31.344
2-Cl-Phe	27.540	32.799	31.344
1-Cl-Ant	27.837	32.896	31.510
2-Cl-Ant	27.837	33.056	31.510
9-Cl-Ant	27.972	33.239	31.906
2,7-Cl_2-Fle	28.232	33.651	31.885
1,2-Br_2-Any	28.376	33.879	32.573
3-Br-Phe	30.036	35.869	34.517
9-Br-Phe	30.345	36.327	35.087
2-Br-Phe	30.345	36.435	35.087
1-Br-Ant	30.517	36.435	35.733
9-Br-Ant	30.779	36.913	35.733
1,5-Cl_2-Ant	32.705	38.285	36.802
9,10-Cl_2-Ant	32.705	38.502	37.149
9,10-Cl_2-Phe	33.060	38.977	37.642
2,7-Br_2-Fle	34.040	40.526	39.052
3-Cl-Flu	34.674	40.845	39.441
1-Cl-Pyr	36.236	43.003	41.517
3-Br-Flu	37.528	44.687	43.059
1,8-Br_2-Ant	38.201	45.229	43.607
1,5-Br_2-Ant	38.201	45.521	44.045
9,10-Br_2-Ant	38.491	45.848	44.538
4-Br-Pyr	38.837	46.551	45.281
9,10-Br_2-Phe	38.875	46.423	45.205
1-Br-Pyr	39.000	46.758	45.489
3,8-Cl_2-Flu	39.690	46.431	45.316
7-Cl-BaA	44.154	52.491	50.593
1,5,9,10-Cl_4-Ant	44.996	54.055	52.093
9-F-BkF	45.534	55.450	52.218
7-Br-BaA	46.590	57.536	55.806
1,6-Br_2-Pyr	46.998	58.203	55.256
6-Cl-BaP	54.056	71.300	55.783

3. Results and discussions

3.1. Comparison of different determination methods

3.1.1. Retention behaviors of X-PAHs in different capillary columns

Three different columns, including non-polar DB-5MS, medium polar DB-35MS, and DB-17MS, were used for X-PAHs separation. The results showed that the separation of most X-PAH isomers could be achieved within 60 min (Table 1). The co-elution of 9-chlorophenanthrene (9-Cl-Phe) and 2-chlorophenanthrene (2-Cl-Phe), 1-chloroanthracene (1-Cl-Ant) and 2-chloroanthracene (2-Cl-Ant), as well as 9-bromophenanthrene (9-Br-Phe) and 2-bromophenanthrene (2-Br-Phe) on both DB-5MS and DB-17MS were observed (Fig. S2). The separation of X-PAH isomers on DB-5MS was similar to a previous work (Jin et al., 2017a). In addition, Cl-/Br-Phe, Cl-/Br-Ant, and Cl_2-/Br_2-Ant could be baseline separated on DB-35MS with only 2-Br-Phe and 1-

bromoanthracene (1-Br-Ant) being co-eluted. Among these three columns, DB-35MS presented the best performance for separation of 34 X-PAHs. Therefore, DB-35MS column was selected for the following study.

3.1.2. Comparison of GC–MS and GC–MS/MS in EI and NCI modes

To compare different ionization techniques, GC–MS and GC–MS/MS with both EI and NCI modes were tested for separation of X-PAHs. Generally, the molecular ions and their halogenated isotopic molecule ions of X-PAHs were observed in both EI and NCI full scan mass spectra (Fig. S3). The response intensity of X-PAHs obtained by NCI was superior to EI, since X-PAHs gave mostly low-mass fragment ions with similar *m/z* values under EI condition, while the presence of halogen atoms gave higher selectivity when using NCI mode (Gonzales, 2011).

However, some isomers of X-PAHs, such as substituted fluorene (Fle), acenaphthene (Ana), and phenanthrene (Phe) were ionized almost exclusively to generate only $[Cl]^-$ (*m/z* 35 and 37) or $[Br]^-$ (*m/z* 79 and 81) in NCI mode, which would increase risk of obtaining false-positive results when using only $[Cl]^-$ or $[Br]^-$ for compound identification. Furthermore, when GC-NCI-MS/MS was used in selected reaction monitoring mode, no molecule ions or specific fragment ions could be selected as precursor ions for some X-PAHs. The optimized precursor-product ion pairs had low responses, or there were no suitable product ions obtained when $[Cl]^-$ or $[Br]^-$ as precursor ions. Therefore, although GC-NCI-MS/MS based methods were used to determine halogenated organics such as organochlorine pesticides in edible oil (Deme et al., 2014), it was not suitable for the identification of X-PAHs, and it would not be discussed in the following sections.

3.1.3. Determination sensitivity of different instruments

To compare the sensitivity of GC–MS and GC–MS/MS for detection of X-PAHs in EI and NCI modes, the instrumental detection limits (IDLs) of GC–MS and GC–MS/MS were determined. A lower concentration of X-PAH standard (0.5 pg/μL) was injected under the identical GC conditions. The IDLs of GC–MS and GC–MS/MS for all the investigated X-PAH isomers were estimated based on a concentration with the signal-to-noise ratio (S/N) of 3 (Sankoda et al., 2013).

As shown in Table 2, the IDLs varied from 0.20–25 pg, from 0.50 to > 500 pg, and from 0.05 to 1 pg for GC-EI-MS, GC-NCI-MS, and GC-EI-MS/MS, respectively. Higher determination sensitivity was achieved under EI mode than NCI mode in tandem mass spectrometry. While, as compared with EI mode, lower ion signal was recorded when the mass spectra operated in NCI mode for several X-PAH isomers such as 9-chlorofluorene (9-Cl-Fle), 9-Cl-Phe, 2-Cl-Phe, 2,7-dichlorofluorene (2,7-Cl_2-Fle), and 9,10-dichlorophenanthrene (9,10-Cl_2-Phe), which were also similar to a previous study (Gonzales, 2011). In particular, the IDLs of Cl-Ant/Phe and Br-Ant/Phe in NCI mode were higher than those in EI mode, while the IDLs of Cl_2-Ant/Phe and Br_2-Ant/Phe in NCI mode were lower than those in EI mode. This might be mainly attributed to high sensitivity of NCI mode for the selectivity of halogenated organic compounds (Buser, 1986; Xu et al., 2019). In addition, the IDLs of 7-chlorobenz[*a*]anthracene (7-Cl-BaA) and 6-chlorobenzo[*a*]pyrene (6-Cl-BaP) in NCI mode were obviously lower than those in EI mode. Even though only a few compounds of X-PAHs were ionized in NCI mode as compared with EI mode, GC-NCI-MS still played an important role in the effective analysis of ultra-trace X-PAHs in practical environmental samples of complex matrices (Gonzales, 2011).

Notably, GC-NCI-MS has been confirmed to be helpful for the thorough screening of samples on halogenated organic compounds (Hauler and Vetter, 2015). Moreover, our results revealed that significant improvements in the IDLs were found for all compounds when working in GC-EI-MS/MS as compared with GC-EI-MS. High selectivity of MS/MS might come from the precise dissociation of the precursor ion, which improved the capability of detector to discriminate a precise product ion, and so it potentially improved instrumental detection limits (Feo et al., 2011). Therefore, GC-EI-MS/MS was suitable for the analysis of all targeted X-PAHs, and a typical chromatogram of standards of X-PAHs is presented in Fig. S4.

Two-dimensional gas chromatography has already been proved to be a very effective separation technique, especially for analyzing complex samples in environments (Ieda et al., 2011; Lacina et al., 2013; Manzano et al., 2012), and tandem mass spectrometry has high sensitivity and selectivity (Ohura et al., 2013). This is because the separating power of a traditional GC is not sufficient to separate every peak in samples from a complex matrix even if the MS/MS is applied for a detector (Hamilton, 2010). Hence, to combine the advantages of GC × GC with tandem mass spectrometry, GC × GC—MS/MS technique was employed in present work. Results showed that GC × GC proved to be efficient for effective separation of 34 X-PAHs (Fig. S5), which were similar to the results reported previously (Hashimoto et al., 2011). As such, the coupling of a GC × GC and an MS/MS could be an effective approach for the complete global detection of X-PAHs (Fig. S5a). For example, 9-Br-Phe and 2-Br-Phe/1-Br-Ant (Fig. S5b and c), and five Cl-Ant/Phe could be completely separated on the second-dimension column by GC × GC. However, due to the high-speed separations in secondary column of GC × GC, the mass detector with a fast acquisition rate is mandatory, which might cause a loss of sensitivity (Adahchour et al., 2005; Giorgia et al., 2010). Therefore, GC × GC might be more suitable than GC for qualitatively screening and discovering compound clusters in complex environmental matrixes. Nevertheless, GC × GC—MS/MS is a powerful technique and can provide superior chromatographic peak capacity and selectivity for the analysis of X-PAHs in complex matrixes.

Table 2
The IDLs (pg) for EI-MS, NCI-MS, and EI-MS/MS analysis methods and the MDLs (pg/g dw) for dust samples.

Compounds	GC-EI-MS		GC-NCI-MS		GC-EI-MS/MS	
	IDL	MDL	IDL	MDL	IDL	MDL
Cl-PAHs						
9-Cl-Fle	0.50	1000	50.0	5000	0.10	4.00
9-Cl-Phe	0.20	45.0	1000	n.d.	0.05	2.00
2-Cl-Phe	0.20	45.0	2000	n.d.	0.05	2.00
1-Cl-Ant	0.20	45.0	5.00	200	0.05	2.00
2-Cl-Ant	0.20	45.0	5.00	200	0.05	2.00
9-Cl-Ant	0.30	45.0	10.0	1000	0.05	2.00
2,7-Cl_2-Fle	0.50	150	2500	n.d.	0.05	2.00
1,5-Cl_2-Ant	5.00	150	0.50	100	0.10	4.00
9,10-Cl_2-Ant	1.00	50.0	0.50	100	0.05	2.00
9,10-Cl_2-Phe	10.0	150	5000	n.d.	0.20	8.00
3-Cl-Flu	1.00	45.0	0.50	1000	0.05	2.00
1-Cl-Pyr	1.00	50.0	0.50	1000	0.05	2.00
3,8-Cl_2-Flu	25.0	60.0	0.50	1000	0.05	2.00
7-Cl-BaA	0.50	40.0	0.50	200	0.05	2.00
1,5,9,10-Cl_4-Ant	5.00	150	0.50	200	1.00	40.0
6-Cl-BaP	0.20	200	0.50	1000	0.05	4.00
Br-PAHs						
5-Br-Ana	0.50	120	10.0	40.0	0.05	2.00
2-Br-Fle	25.0	100	2500	n.d.	0.05	2.00
1,2-Br_2-Any	25.0	150	0.50	1000	0.50	20.0
3-Br-Phe	5.00	50.0	200	n.d.	0.05	2.00
9-Br-Phe	5.00	50.0	200	n.d.	0.05	2.00
2-Br-Phe [b]	5.00	30.0	500	n.d.	0.05	2.00
1-Br-Ant [b]	5.00	30.0	500	n.d.	0.05	2.00
9-Br-Ant	5.00	50.0	500	n.d.	0.10	4.00
2,7-Br_2-Fle	10.0	200	200	n.d.	0.20	8.00
3-Br-Flu	0.50	200	0.50	1000	0.10	4.00
1,8-Br_2-Ant	5.00	150	0.50	1000	0.50	20.0
1,5-Br_2-Ant	5.00	150	0.50	1000	0.50	20.0
9,10-Br_2-Ant	5.00	150	0.50	1000	0.50	20.0
9,10-Br_2-Phe	10.0	100	100.0	n.d.	0.50	20.0
4-Br-Pyr	0.50	200	200	n.d.	0.10	4.00
1-Br-Pyr	0.50	200	200	n.d.	0.10	4.00
1,6-Br_2-Pyr	1.00	100	25.0	1000	0.50	20.0
7-Br-BaA	5.00	180	50.0	1000	0.05	2.00

[a]Not detected. [b] Co-elution of isomers.

3.1.4. Validation of the developed method and matrix effect evaluation

To evaluate the performance of the developed method for the analysis of all targeted X-PAHs by GC-EI-MS/MS, the linearity, recovery, precision, and sensitivity were examined (Tables S3 and S4). Calibration curves were constructed for all X-PAHs and the linear calibration ranges varied from 0.5–200 pg/μL at eight concentrations. The limit of quantification (LOQ) was 0.10 ng/g dw based on the lowest concentration of the calibration curve. Good linearity was achieved within the interval studied with correlation coefficients ranging between 0.9912 and 0.9999 (Table S3). In this study, samples of procedural blanks and spiked inert sorbent material were also performed with each batch of samples and none of the target X-PAHs was detected in the procedural blanks. In addition, the satisfactory recoveries of 56.9 %–130.6 % and 67.3 %–120.2 % were obtained by spiked X-PAHs in the sorbent material with concentrations of 200 and 1000 pg/g dw, respectively. The precisions of the method, obtained as the relative standard deviations (RSDs) of analyte recoveries, were 0.3 %–21.6 % in all spiking experiments (Table S4). The same criteria as IDLs were used to determine the method detection limits (MDLs) from spiked sorbent material and the highest sensitivity was achieved using GC-EI-MS/MS method, with MDLs (varied from 2.00–20.0 pg/g dw) one to two magnitude lower than those with GC-EI-MS (from 45 to > 200 pg/g dw). However, when using GC-NCI-MS method, some compounds such as Cl-Phe and Br-Phe were not detectable even in high spike levels (1000 pg/g dw). To evaluate matrix effect, an inert sorbent material and SRM 2585 were spiked at 1000 pg/g dw and analyzed in parallel to test for matrix effects using recoveries. As Fig. S6 shows, the recoveries of the analytes ranged from 69.3%–122.9% for the inert sorbent material and from 64.1%–120.7% for SRM 2585 with RSDs below 12 % and 15 % in the two matrices, respectively. The satisfactory recoveries and RSDs of the analytes in the two matrices indicated that the matrix effects could be ignored.

As well known, in the analysis of persistent organic pollutants at ultra-trace levels (pg/μL level and lower), the GC-HRMS based methods were generally recognized as the "gold standard". Therefore, in this study, the MDLs of the X-PAH isomers determined using GC-EI-MS/MS were compared with those using GC-HRMS. The present MDLs of Σ_{16}Cl-PAHs determined using GC-EI-MS/MS for indoor dust samples were slightly higher than the MDLs of Σ_{20}Cl-PAHs using GC-HRMS reported in a previous study, in which the MDLs were 0.5–8.7 pg/g dw for sediments (Horii et al., 2009). However, the MDLs of 9-Cl-Phe (3.0 pg/g dw), 9-chloroanthracene (9-Cl-Ant) (2.4 pg/g dw), 9,10-dichloroanthracene (9,10-Cl_2-Ant) (3.1 pg/g dw), 1-chloropyrene (1-Cl-Pyr) (3.2 pg/g dw), and 3-chlorofluoranthene (3-Cl-Flu) (1.4 pg/g dw) in this study were comparable to our results using GC-EI-MS/MS. Considering higher sensitivity, relative easier in operation and maintenance, together with its cheaper, GC-EI-MS/MS based methods would be preferred for the routine determination of X-PAHs in the samples from environments.

3.2. Profiles of X-PAHs in indoor dust samples and SRM 2585

The analysis of individual Cl-PAH and Br-PAH isomer in indoor dust samples and SRM 2585 are listed in Table 3. The levels of Σ_{16}Cl-PAHs and Σ_{18}Br-PAHs ranged from 7.91–137 ng/g dw and from 8.80–399 ng/g dw in the indoor dust, respectively. As observed, the concentrations of chlorine-substituted isomers were slightly lower than that of bromine-substituted groups, which might be due to the large number of bromine sources, such as bromine flame retardant, were released during the e-waste dismantling process, makes it relatively easier to generate of Br-PAHs (Liu et al., 2019; Nishimura et al., 2017). Significantly higher concentrations of Br-PAHs and Cl-PAHs were also observed in e-waste dismantling workshops (BW, EW and RW) than those in OA. This further confirmed that the e-waste disposal processes is the main factor influence the formation of X-PAHs. As being reported by previous studies (Jin et al., 2017b; Ma et al., 2009; Xu et al., 2018), during the industrial thermal processes of e-waste disposal, fuel acts as a carbon source to form organic contaminants and their precursors. Organic impurities, such as polyvinyl chloride (Zheng et al., 2008) and flame retardants (Paine et al., 2014), contained in e-waste materials (e.g., printed circuit board, electronic parts and components, and electric appliance outer) could provide halogens for Cl-/Br-PAH formation. Finally, certain metals from e-waste disposal might catalyze Cl-/Br-PAH formation at appropriate temperatures in the cooling stages (Nganai et al., 2011; Xu et al., 2018). Therefore, Cl-/Br-PAH might be formed and released from the industrial thermal processes of e-waste disposal, and then adhere to the dusts and finally settle down. The treatment process and dismantling temperature are quite different from various workshops, which would result in different emission profiles of X-PAHs in dusts. The low-ring X-PAHs (Cl-Phe/-Ant and Cl_2-Phe) were mainly Cl-PAHs, and the high-ring X-PAHs (Br-Pyr and Br-BaA) were mainly Br-PAHs (Fig. 1). This result might be due to the relatively higher air stability and photostability of low-ring Cl-PAHs against that of high-ring isomers (Ohura et al., 2004, 2005), and indicates that Cl-PAHs and Br-PAHs might behave differently in the ambient environment and the main source of Cl-PAHs might not be the same as that of Br-PAHs. As mentioned in previous studies (Vuong et al., 2020; Wang et al., 2003), HCl produced by the PVC combustion could be transformed into Cl_2 and participated in the chlorination of PAHs, therefore, Cl-PAHs could be formed during the combustion process of PVC of e-wastes. For Br-PAHs,

Table 3
Mean concentrations (ng/g dw) of X-PAHs in dust samples measured by GC-EI-MS/MS (EW: e-waste dismantling workshop, n = 5; RW: raw materials crushing workshop, n = 3; BW: secondary copper blast furnace workshop, n = 3; OA: office building area, n = 2; RA: residential area, n = 2) and SRM 2585.

Compounds	EW	RW	BW	OA	RA	SRM
Cl-PAHs						
9-Cl-Fle	n.d.	n.d.	n.d.	n.d.[a]	n.d.	n.d.
9-Cl-Phe	1.81	2.67	6.34	0.97	0.52	37.9
2-Cl-Phe	38.4	4.50	2.64	0.38	28.5	6.02
1-Cl-Ant	n.d.	n.d.	n.d.	n.d.	28.0	5.74
2-Cl-Ant	46.7	5.14	3.83	0.81	30.4	4.47
9-Cl-Ant	15.6	2.46	1.48	n.d.	17.3	7.39
2,7-Cl_2-Fle	n.d.	0.80	n.d.	n.d.	n.d.	0.01
1,5-Cl_2-Ant	7.00	1.56	4.31	< LOQ	9.87	7.40
9,10-Cl_2-Ant	0.49	< LOQ	0.83	< LOQ	0.72	0.49
9,10-Cl_2-Phe	21.5	6.83	14.6	0.33	17.2	6.40
3-Cl-Flu	1.92	1.95	4.34	0.59	0.50	3.02
1-Cl-Pyr	2.45	3.85	9.68	1.92	2.55	32.1
3,8-Cl_2-Flu	n.d.	n.d.	n.d.	n.d.	n.d.	< LOQ
7-Cl-BaA	1.51	1.67	2.51	0.34	1.86	2.30
1,5,9,10-Cl_4-Ant	n.d.	n.d.	n.d.	n.d.	n.d.	n.d.
6-Cl-BaP	n.d.	3.67	3.25	2.56	n.d.	n.d.
Σ_{16}Cl-PAHs	137	35.1	53.8	7.91	137	113
Br-PAHs						
5-Br-Ana	n.d.	n.d.	n.d.	< LOQ	n.d.	6.28
2-Br-Fle	n.d.	n.d.	n.d.	n.d.	n.d.	< LOQ
1,2-Br_2-Any	4.98	11.4	31.7	10.0	1.93	0.42
3-Br-Phe	0.54	0.85	1.16	< LOQ	n.d.	n.d.
9-Br-Phe	6.66	3.28	5.08	< LOQ	8.63	1.26
2-Br-Phe[b]	n.d.	9.50	n.d.	n.d.	n.d.	n.d.
1-Br-Ant[b]	n.d.	9.50	n.d.	n.d.	n.d.	n.d.
9-Br-Ant	3.10	8.63	1.27	0.43	0.94	0.35
2,7-Br_2-Fle	6.70	6.15	n.d.	n.d.	5.10	0.08
3-Br-Flu	3.72	12.2	14.4	1.28	0.27	0.10
1,8-Br_2-Ant	5.30	2.06	1.47	n.d.	< LOQ	n.d.
1,5-Br_2-Ant	n.d.	n.d.	n.d.	n.d.	n.d.	0.11
9,10-Br_2-Ant	5.58	1.59	< LOQ	n.d.	0.39	n.d.
4-Br-Pyr	3.34	1.57	28.8	7.35	n.d.	< LOQ
9,10-Br_2-Phe	n.d.	0.74	1.61	n.d.	0.30	n.d.
1-Br-Pyr	1.21	268	42.3	4.88	0.29	< LOQ
1,6-Br_2-Pyr	n.d.	44.4	22.7	3.02	n.d.	0.20
7-Br-BaA	18.8	19.3	1.18	< LOQ	7.84	< LOQ
Σ_{18}Br-PAHs	60.0	399	152	27.0	25.7	8.80

[a] Not detected; [b] Co-elution of isomers; [c] The concentrations of X-PAHs were lower than LOQ.

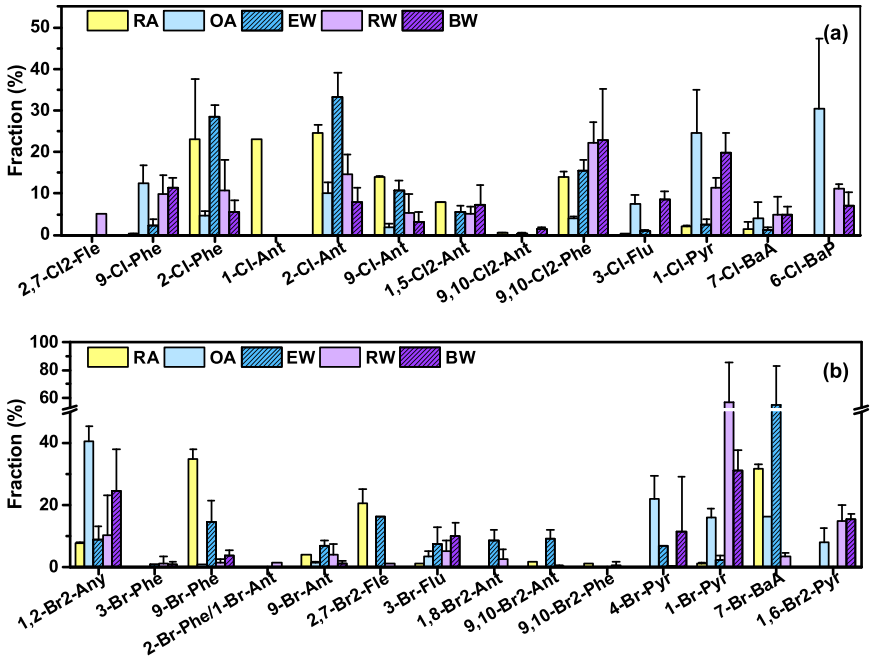

Fig. 1. Congener and homologue distributions of Cl-PAHs and Br-PAHs in indoor dust samples (RA: residential area, n = 2; OA: office building area, n = 2; EW: e-waste dismantling workshop, n = 5; RW: raw materials crushing workshop, n = 3; BW: secondary copper blast furnace workshop, n = 3). (a) Congener distributions of Cl-PAHs; (b) Congener distributions of Br-PAHs.

they might be by-products of thermochemical reactions generated by fly ash-mediated heterogenous reactions (Wu et al., 2019), or their formation might be through a precursor mechanism from highly BFRs (e.g. DBDPE) readily available in e-wastes (Tue et al., 2017). The dominant Cl-PAH isomer was 2-Cl-Ant, with concentrations of 0.81–46.7 ng/g dw, followed by 2-Cl-Phe, 9,10-Cl_2-Phe, 1-Cl-Pyr, and 9-Cl-Phe. 1-Cl-Ant was only detected in RA and SRM, suggesting that the dust samples in these two sites may have similar dust characteristics. 1-Cl-Pyr was detected in dust samples in all sites in our study. This result is similar to other studies of 1-Cl-Pyr commonly reported in the environment (Horii et al., 2008; Ma et al., 2009). The dominant Br-PAH isomer was 1-bromopyrene (1-Br-Pyr) with a concentration ranging from < LOQ to 268 ng/g dw, while 1,6-dibromopyrene (1,6-Br_2-Pyr), 1,2-dibromoacenaphthylene (1,2-Br_2-Any), 7-bromobenz[*a*]anthracene (7-Br-BaA), and 4-bromopyrene(4-Br-Pyr) were also frequently detected. The high-ring Cl-PAHs (1-Cl-Pyr, 7-Cl-BaA and 6-Cl-BaP) and Br-PAHs (1-Br-Pyr and 1,6-Br_2-Pyr) found in indoor dust samples were dominant at the industrial park including the RW and BW sites, which were might be related to the different e-waste dismantling techniques used in those two workshops.

Compared with other studies, 2-Cl-Ant, 9-Cl-Ant, 9,10-Cl_2-Ant, 3-Cl-Flu, 3,8-dichlorofluoranthene (3,8-Cl_2-Flu), 1-Cl-Pyr, 7-Cl-BaA, 6-Cl-BaP were all found in indoor dust Guangzhou (Gonzales, 2011). 1-Cl-Pyr and 3-Cl-Flu as the major Cl-PAH isomers in indoor dust from Guangzhou (Gonzales, 2011) and e-waste recycling facility (Ma et al., 2009), were similar to those in our study. For Br-PAHs, the present concentrations were lower than those in the fly ash (< 0.14–1235 ng/g) (Horii et al., 2008) and those in soils and sediments (3.14–914 ng/g) (Ohura et al., 2013). However, the dominant Br-PAH isomers in indoor dust in our work were not previously published in the indoor dust samples, but has been reported in soils from Vietnam, the Philippines, and Ghana (Nishimura et al., 2017; Ohura et al., 2013), sediments from America and China (Ohura et al., 2013; Sun et al., 2011), and atmospheric and stack gas samples from China (Jin et al., 2017a). For example, Horri et al. have reported that 1-Br-Pyr was the main Br-PAH isomer found in the fly ash in waste incinerator from South Korea (Horii et al., 2008), which was similar to the present result. The predominant Cl-PAH isomers in dust samples were similar among different regions, this might result from similar sources or have a similar formation process. Further investigation is needed to clarify the specific formation mechanism.

Finally, the established method was further applied to analyze the concentrations of Σ_{16}Cl-PAHs and Σ_{18}Br-PAHs in SRM 2585 in dust samples (Table 3). Due to their similarities in chemical structure and properties, the concentrations of 16 United States Environmental Protection Agency priority PAHs were also determined simultaneously with their halogenated derivatives. The concentrations of individual PAH isomers in this study (Table S5) agreed well with the certified values of PAHs provided by NIST and literature (Poster et al., 2007). The results suggested that the developed method was robust for the analysis of both PAHs and X-PAHs in indoor dust. Moreover, the present results showed that the levels of Σ_{16}Cl-PAHs and Σ_{18}Br-PAHs in SRM 2585 were 113 and 8.80 ng/g dw, respectively. This is the first report on the concentrations and distribution of X-PAHs in SRM 2585. The results contributed to further understand human health effects in relation to X-PAHs associated with indoor dust to some extent. However, the measured values of X-PAHs in our study were noncertified values and provided with associated uncertainties which reflected only measurement precision and did not included all sources of uncertainty. Therefore, further analysis and research of X-PAHs in indoor dust as well as SRM 2585 are needed.

3.3. Human exposure risk

Based on the toxic potencies relative to BaP activity (REP_{BaP}), TEQs were used to assess the human exposure risk to X-PAHs in e-waste dismantling workshops. The detailed calculation method is provided in SI (Eq. S1). REP_{BaP} and mean TEQs of X-PAHs at all sampling sites are presented in Table S6. The $TEQ_{Cl\text{-}PAHs}$ and $TEQ_{Br\text{-}PAHs}$ ranged from 16.1–176 pg·TEQ/g and from 3.33–453 pg·TEQ/g in indoor dusts, respectively. The EW site showed obviously higher mean $TEQ_{Cl\text{-}PAHs}$ (176 pg·TEQ/g) than those at other sites, while the RW site showed significantly higher mean $TEQ_{Br\text{-}PAHs}$ (453 pg·TEQ/g). 9,10-Cl_2-Phe, 2-Cl-Ant and 7-Cl-BaA collectively made up the predominance of total $TEQ_{Cl\text{-}PAH}$ in dust. 7-Br-BaA and 1-Br-Pyr were major contributors to the total $TEQ_{Br\text{-}PAH}$ in dust samples.

In general, the mean $TEQ_{Cl\text{-}PAH}$ at all sites (OA: 16.1 pg·TEQ/g; EW: 176 pg·TEQ/g; RA: 139 pg·TEQ/g; RW: 69.9 pg·TEQ/g; BW: 120 pg·TEQ/g) in our study were lower than that in workshop-floor dust (518 pg·TEQ/g) from e-waste recycling facility (Ma et al., 2009), but

was 1- to 11-fold higher than that in fly ash (15.6 pg·TEQ/g) from waste incinerator (Horii et al., 2008). The mean $TEQ_{Br\text{-}PAH}$ at EW site (267 pg·TEQ/g) and RW site (453 pg·TEQ/g) were all higher than those in soil collected at open e-waste burning sites from Vietnam (120 pg·TEQ/g), the Philippines (7.50 pg·TEQ/g) and Ghana (120 pg·TEQ/g) (Nishimura et al., 2017). Similar to our study, 2-Cl-Ant and 7-Br-BaA were also major contributor of $TEQ_{Cl\text{-}PAH}$ and $TEQ_{Br\text{-}PAH}$, respectively, in soil from an urbanized region in China (Ni and Zeng, 2012).

The human exposures to Cl-PAHs and Br-PAHs in the e-waste dismantling industrial park and its surrounding area by dust ingestion were evaluated and calculated based on their TEQ concentrations (Eq. S2). Average daily intake (DI) of Cl-PAHs and Br-PAHs were 7.77 − 19.6 and 5.18 − 50.3 fg TEQ kg^{-1} d^{-1}, respectively, for the workers in EW, RW and BW, and 3.56 − 30.9 and 0.74 − 25.1 fg TEQ kg^{-1} d^{-1}, respectively, for residents in OA and RA. The $DI_{Cl\text{-}PAHs}$ and $DI_{Br\text{-}PAHs}$ were significantly lower than the tolerable daily intake recommended by the WHO (1 − 4 pg TEQ kg^{-1} d^{-1}) for dioxin (Jin et al., 2017b). Moreover, the $DI_{Cl\text{-}PAHs}$ via dust ingestion for workers from EW, RW and BW was all lower than $DI_{Cl\text{-}PAHs}$ via air inhalation for workers from the secondary copper smelters (121 fg TEQ kg^{-1} d^{-1}), while the $DI_{Br\text{-}PAHs}$ via dust ingestion for workers from EW, RW and BW was all significantly higher than $DI_{Br\text{-}PAHs}$ (1.7 fg TEQ kg^{-1} d^{-1}) via air inhalation for workers (Jin et al., 2017b). Human exposure to Br-PAHs adsorbed to dust through dust ingestion for workers should be a cause for concern.

In summary, DI of X-PAHs via dust ingestion based on their TEQs in indoor dusts from e-waste dismantling workshop were calculated to assess human exposure risk in our study. However, due to the lack of available data for Br-PAHs and Cl-PAHs in indoor dust samples as well as REP_{BaP} for calculating TEQs of X-PAHs, more studies on toxic potencies of X-PAHs are required in the future in order to accurately estimate the human exposure risk due to X-PAHs.

4. Conclusions

In our study, the best selectivity and sensitivity for analysis of X-PAHs were found when GC–MS/MS in EI mode, exhibiting detection limits comparable to GC-HRMS. A significant decrease of matrix interferences was found, which provides higher confidence for using GC-EI-MS/MS to qualitatively and quantitatively analyze X-PAHs in indoor dusts in e-waste dismantling workshops and SRM 2585. The concentrations of Σ_{16}Cl-PAHs were lower than those of Σ_{18}Br-PAHs. The EW site showed higher mean $TEQ_{Cl\text{-}PAHs}$ while the RW site showed higher mean $TEQ_{Br\text{-}PAHs}$. DI via dust ingestion of X-PAHs was estimated, which suggested that X-PAHs could pose a potential health risk to human. Our results demonstrated the widespread occurrence of X-PAHs in the settled dust, and further research is needed regarding their potential toxic effects.

CRediT authorship contribution statement

Jian Tang: Methodology, Formal analysis, Writing - original draft. **Shengtao Ma:** Methodology, Data curation. **Ranran Liu:** Methodology, Formal analysis. **Congcong Yue:** Methodology, Formal analysis. **Guiying Li:** Writing - review & editing. **Yingxin Yu:** Visualization, Investigation. **Yan Yang:** Validation. **Taicheng An:** Conceptualization, Supervision.

Declaration of Competing Interest

The authors declare that they have no known competing financial interests or personal relationships that could have appeared to influence the work reported in this paper.

Acknowledgements

This work was supported by the National Natural Science Foundation of China (41731279, 41425015, 41977303 and 41703092), Local Innovative and Research Teams Project of Guangdong Pearl River Talents Program (2017BT01Z032), and the Innovation Team Project of Guangdong Provincial Department of Education (2017KCXTD012). We thank Prof. Minghui Zheng in Research Center for Eco-Environmental Sciences, Chinese Academy of Sciences for his generous providing several Cl-/Br-PAH standards for us.

Appendix A. Supplementary data

Supplementary material related to this article can be found, in the online version, at doi:https://doi.org/10.1016/j.jhazmat.2020.122573.

References

Adahchour, M., Brandt, M., Baier, H.U., Vreuls, R.J.J., Batenburg, A.M., Brinkman, U.A.T., 2005. Comprehensive two-dimensional gas chromatography coupled to a rapid-scanning quadrupole mass spectrometer: principles and applications. J. Chromatogr. A 1067, 245–254.

Buser, H.R., 1986. Selective detection of brominated aromatic compounds using gas chromatography/negative chemical ionization mass spectrometry. Anal. Chem. 58, 2913–2919.

Chen, H., Ma, S., Yu, Y., Liu, R., Li, G., Huang, H., An, T., 2019. Seasonal profiles of atmospheric PAHs in an e-waste dismantling area and their associated health risk considering bioaccessible PAHs in the human lung. Sci. Total Environ. 683, 371–379.

Deme, P., Azmeera, T., Devi, B.L.A.P., Jonnalagadda, P.R., Prasad, R.B.N., Sarathi, U.V.R.V., 2014. An improved dispersive solid-phase extraction clean-up method for the gas chromatography-negative chemical ionisation tandem mass spectrometric determination of multiclass pesticide residues in edible oils. Food Chem. 142, 144–151.

Fan, Y., Zhang, H., Wang, D., Ren, M., Zhang, X., Wang, L., Chen, J., 2017. Simultaneous determination of chlorinated aromatic hydrocarbons in fly ashes discharged from industrial thermal processes. Anal. Methods 9, 5198–5203.

Feo, M.L., Eljarrat, E., Barcelo, D., 2011. Performance of gas chromatography/tandem mass spectrometry in the analysis of pyrethroid insecticides in environmental and food samples. Rapid Commun. Mass Spectrom. 25, 869–876.

Giorgia, P., Peter Quinto, T., Carla, R., Lanfranco, C., Paola, D., Giovanni, D., Luigi, M., 2010. Evaluation of a rapid-scanning quadrupole mass spectrometer in an apolar × ionic-liquid comprehensive two-dimensional gas chromatography system. Anal. Chem. 82, 8583–8590.

Gonzales, L.R., 2011. Trace Analysis of Halogenated Polycyclic Aromatic Hydrocarbons From an Electronic Waste Recycling Area and Guangzhou. Oregon State University, China.

Haglund, P., Alsberg, T., Bergman, A., Bo, J., 1987. Analysis of halogenated polycyclic aromatic hydrocarbons in urban air, snow and automobile exhaust. Chemosphere 16, 2441–2450.

Hamilton, J.F., 2010. Using comprehensive two-dimensional gas chromatography to study the atmosphere. J. Chromatogr. Sci. 48, 274–282.

Hashimoto, S., Takazawa, Y., Fushimi, A., Tanabe, K., Shibata, Y., Ieda, T., Ochiai, N., Kanda, H., Ohura, T., Tao, Q., 2011. Global and selective detection of organohalogens in environmental samples by comprehensive two-dimensional gas chromatography–tandem mass spectrometry and high-resolution time-of-flight mass spectrometry. J. Chromatogr. A 1218, 3799–3810.

Hauler, C., Vetter, W., 2015. A non-targeted gas chromatography/electron capture negative ionization mass spectrometry selected ion monitoring screening method for polyhalogenated compounds in environmental samples. Rapid Commun. Mass Spectrom. 29, 619–628.

Horii, Y., Ok, G., Ohura, T., Kannanct, K., 2008. Occurrence and profiles of chlorinated and brominated polycyclic aromatic hydrocarbons in waste incinerators. Environ. Sci. Technol. 42, 1904–1909.

Horii, Y., Ohura, T., Yamashita, N., Kannan, K., 2009. Chlorinated polycyclic aromatic hydrocarbons in sediments from industrial areas in Japan and the United States. Arch. Environ. Contam. Toxicol. 57, 651–660.

Horii, Y., Khim, J.S., Higley, E.B., Giesy, J.P., Ohura, T., Kannan, K., 2013. Relative potencies of individual chlorinated and brominated polycyclic aromatic hydrocarbons for induction of aryl hydrocarbon receptor-mediated responses. Environ. Sci. Technol. 43, 2159–2165.

Ieda, T., Ochiai, N., Miyawaki, T., Ohura, T., Horii, Y., 2011. Environmental analysis of chlorinated and brominated polycyclic aromatic hydrocarbons by comprehensive two-dimensional gas chromatography coupled to high-resolution time-of-flight mass spectrometry. J. Chromatogr. A 1218, 3224–3232.

Jin, R., Liu, G., Zheng, M., Fiedler, H., Jiang, X., Yang, L., Wu, X., Xu, Y., 2017a. Congener-specific determination of ultratrace levels of chlorinated and brominated polycyclic aromatic hydrocarbons in atmosphere and industrial stack gas by isotopic dilution gas chromatography/high resolution mass spectrometry method. J. Chromatogr. A 1509, 114–122.

Jin, R., Liu, G., Zheng, M., Jiang, X., Zhao, Y., Yang, L.L., Wu, X., Xu, Y., 2017b.

Secondary copper smelters as sources of chlorinated and brominated polycyclic aromatic hydrocarbons. Environ. Sci. Technol. 51, 7945–7953.
Jin, R., Zheng, M.H., Lammel, G., Bandowe, B.A.M., Liu, G.R., 2020. Chlorinated and brominated polycyclic aromatic hydrocarbons: sources, formation mechanisms, and occurrence in the environment. Prog. Energy Combust. Sci. 76, 20.
Lacina, P., Mravcova, L., Vavrova, M., 2013. Application of comprehensive two-dimensional gas chromatography with mass spectrometric detection for the analysis of selected drug residues in wastewater and surface water. J. Environ. Sci.-China 25, 204–212.
Liu, R., Ma, S., Li, G., Yu, Y., An, T., 2019. Comparing pollution patterns and human exposure to atmospheric PBDEs and PCBs emitted from different e-waste dismantling processes. J. Hazard. Mater. 369, 142–149.
Ma, J., Horii, Y., Cheng, J., Wang, W., Wu, Q., Ohura, T., Kannan, K., 2009. Chlorinated and parent polycyclic aromatic hydrocarbons in environmental samples from an electronic waste recycling facility and a chemical industrial complex in China. Environ. Sci. Technol. 43, 643–649.
Ma, J., Chen, Z., Wu, M., Feng, J., Horii, Y., Ohura, T., Kannan, K., 2013. Airborne PM2.5/PM10-associated chlorinated polycyclic aromatic hydrocarbons and their parent compounds in a suburban area in Shanghai, China. Environ. Sci. Technol. 47, 7615–7623.
Manzano, C., Hoh, E., Simonich, S.L., 2012. Improved separation of complex polycyclic aromatic hydrocarbon mixtures using novel column combinations in GC × GC/ToF-MS. Environ. Sci. Technol. 46, 7677–7684.
Miren, P.A., Jobst, K.J., Ralph, R., Li, S., Robert, M.C., Helm, P.A., Reiner, E.J., 2014. Identification of potential novel bioaccumulative and persistent chemicals in sediments from Ontario (Canada) using scripting approaches with GC×GC-TOF MS analysis. Environ. Sci. Technol. 48, 9591–9599.
Mo, L.G., Ma, S.T., Li, H.R., Yu, Z.Q., Sheng, G.Y., Fu, J.M., 2013. Determination of chlorinated-and brominated-polycyclic aromatic hydrocarbons in soil samples by gas chromatography coupled with triple quadrupole mass spectrometry. Chinese J. Anal. Chem. 41, 1825–1830.
Nganai, S., Lomnicki, S.M., Dellinger, B., 2011. Formation of PCDD/Fs from the copper oxide-mediated pyrolysis and oxidation of 1,2- dichlorobenzene. Environ. Sci. Technol. 45, 1034–1040.
Ni, H.G., Zeng, E.Y., 2012. Environmental and human exposure to soil chlorinated and brominated polycyclic aromatic hydrocarbons in an urbanized region. Environ. Toxicol. Chem. 31, 1494–1500.
Nilsson, U.L., Oestman, C.E., 1993. Chlorinated polycyclic aromatic hydrocarbons: method of analysis and their occurrence in urban air. Environ. Sci. Technol. 27, 1826–1831.
Nishimura, C., Horii, Y., Tanaka, S., Asante Jr, K.A., Viet, B.F., Itai, P.H., Takigami, T., Tanabe, H., Fujimori T, S., 2017. Occurrence, profiles, and toxic equivalents of chlorinated and brominated polycyclic aromatic hydrocarbons in E-waste open burning soils. Environ. Pollut. 225, 252–260.
NIST, 2010. Standard Reference Material 2585 (Organic Contaminantsin House Dust). https://www-s.nist.gov/srmors/certificates/2585.pdf?CFID=8005724&CFTOKEN=6055912e137af10-FF97E690-CC33-18B9D70EC59033806ADC&jsessionid=f0309c4118606be2b0d7663932533b401473.
Ohura, T., 2007. Environmental behavior, sources, and effects of chlorinated polycyclic aromatic hydrocarbons. Sci. World J. 7, 372–380.
Ohura, T., Kitazawa, A., Amagai, T., 2004. Seasonal variability of 1-chloropyrene on atmospheric particles and photostability in toluene. Chemosphere 57, 831–837.
Ohura, T., Kitazawa, A., Amagai, T., Makino, M., 2005. Occurrence, profiles, and photostabilities of chlorinated polycyclic aromatic hydrocarbons associated with particulates in urban air. Environ. Sci. Technol. 39, 85–91.
Ohura, T., Morita, M., Makino, M., Amagai, T., Shimoi, K., 2007. Aryl hydrocarbon receptor-mediated effects of chlorinated polycyclic aromatic hydrocarbons. Chem. Res. Toxicol. 20, 1237–1241.
Ohura, T., Fujima, S., Amagai, T., Shinomiya, M., 2008. Chlorinated polycyclic aromatic hydrocarbons in the atmosphere: seasonal levels, gas-particle partitioning, and origin. Environ. Sci. Technol. 42, 3296–3302.
Ohura, T., Sawada, K., Amagai, T., Shinomiya, M., 2009. Discovery of novel halogenated polycyclic aromatic hydrocarbons in urban particulate matters: occurrence, photostability, and AhR activity. Environ. Sci. Technol. 43, 2269–2275.
Ohura, T., Morita, M., Kurutoniwa, R., Amagai, T., Sakakibara, H., Shimoi, K., 2010. Differential action of chlorinated polycyclic aromatic hydrocarbons on aryl hydrocarbon receptor-mediated signaling in breast cancer cells. Environ. Toxicol. 25, 180–187.
Ohura, T., Yamamoto, T., Higashino, K., Sasaki, Y., 2013. Halogenated PAH Contamination in Urban Soils. Springer, Netherlands.
Ohura, T., Sakakibara, H., Watanabe, I., Shim, W.J., Manage, P.M., Guruge, K.S., 2015. Spatial and vertical distributions of sedimentary halogenated polycyclic aromatic hydrocarbons in moderately polluted areas of Asia. Environ. Pollut. 196, 331–340.
Ohura, T., Kamiya, Y., Ikemori, F., 2016. Local and seasonal variations in concentrations of chlorinated polycyclic aromatic hydrocarbons associated with particles in a Japanese megacity. J. Hazard. Mater. 312, 254–261.
Paine, M.R.L., Rae, I.D., Blanksby, S.J., 2014. Direct detection of brominated flame retardants from plastic e-waste using liquid extraction surface analysis mass spectrometry. Rapid Commun. Mass Spectrom. 28, 1203–1208.
Petros, D.C., Alex, B., Saer, S., Juliane, H., Rebecca, R., Jimmy, W., Jonas, G., J Samuel, A., 2015. GC×GC quantification of priority and emerging nonpolar halogenated micropollutants in all types of wastewater matrices: analysis methodology, chemical occurrence, and partitioning. Environ. Sci. Technol. 49, 7914–7925.
Poster, D.L., Kucklick, J.R., Schantz, M.M., Vander Pol, S.S., Leigh, S.D., Wise, S.A., 2007. Development of a house dust standard reference material for the determination of organic contaminants. Environ. Sci. Technol. 41, 2861–2867.
Sankoda, K., Kuribayashi, T., Nomiyama, K., Shinohara, R., 2013. Occurrence and source of chlorinated polycyclic aromatic hydrocarbons (Cl-PAHs) in tidal flats of the Ariake Bay, Japan. Environ. Sci. Technol. 47, 7037–7044.
Stapleton, H.M., Harner, T., Shoeib, M., Keller, J.M., Schantz, M.M., Leigh, S.D., Wise, S.A., 2006. Determination of polybrominated diphenyl ethers in indoor dust standard reference materials. Anal. Bioanal. Chem. 384, 791–800.
Sun, J.L., Ni, H.G., Zeng, H., 2011. Occurrence of chlorinated and brominated polycyclic aromatic hydrocarbons in surface sediments in Shenzhen, South China and its relationship to urbanization. J. Environ. Monit. 13, 2775–2781.
Sun, J.L., Zeng, H., Ni, H.G., 2013. Halogenated polycyclic aromatic hydrocarbons in the environment. Chemosphere 90, 1751–1759.
Takeshi, O., Maki, M., Masakazu, M., Takashi, A., Kayoko, S., 2007. Aryl hydrocarbon receptor-mediated effects of chlorinated polycyclic aromatic hydrocarbons. Chem. Res. Toxicol. 20, 1237–1241.
Tue, N.M., Goto, A., Takahashi, S., Itai, T., Asante, K.A., Nomiyama, K., Tanabe, S., Kunisue, T., 2017. Soil contamination by halogenated polycyclic aromatic hydrocarbons from open burning of e-waste in Agbogbloshie (Accra, Ghana). J. Mater. Cycles Waste Manag. 19, 1324–1332.
Vuong, Q.T., Kim, S.-J., Nguyen, T.N.T., Thang, P.Q., Lee, S.-J., Ohura, T., Choi, S.-D., 2020. Passive air sampling of halogenated polycyclic aromatic hydrocarbons in the largest industrial city in Korea: spatial distributions and source identification. J. Hazard. Mater. 382, 121238.
Wang, D., Xu, X., Chu, S., Zhang, D., 2003. Analysis and structure prediction of chlorinated polycyclic aromatic hydrocarbons released from combustion of polyvinylchloride. Chemosphere 53, 495–503.
Wu, X., Wu, G., Xie, J., Wang, Q., Liu, G., Liu, W., Yang, L., Zheng, M., 2019. Thermochemical formation of multiple unintentional persistent organic pollutants on metallurgical fly ash and their correlations. Chemosphere 226, 492–501.
Xu, Y., Yang, L., Zheng, M., Jin, R., Wu, X., Li, C., Liu, G., 2018. Chlorinated and brominated polycyclic aromatic hydrocarbons from metallurgical plants. Environ. Sci. Technol. 52, 7334–7342.
Xu, J., Guo, W., Wei, L., Gao, Y., Zhang, H., Zhang, Y., Sun, M., Chen, J., 2019. Validation of a HRGC-ECNI/LRMS method to monitor short-chain chlorinated paraffins in human plasma. J. Environ. Sci. 75, 289–295.
Zheng, G.J., Leung, A.O.W., Jiao, L.P., Wong, M.H., 2008. Polychlorinated dibenzo-p-dioxins and dibenzofurans pollution in China: sources, environmental levels and potential human health impacts. Environ. Int. 34, 1050–1061.